Reaction of 4 with Br_2. As with the analogous reaction for **1**, a 5-mm NMR tube was loaded with 0.035 g of Tp^*PtMe_3, and 3 equiv or more of Br_2 was injected. The ^1H NMR spectrum showed only changes consistent with bromination of the 4-H position of the three pyrazolyl rings. ^1H NMR ($CDCl_3$), δ: 2.61 (9 H, s), 2.41 (9 H, s), 1.50 (9 H, m, $^2J_{Pt-H}$ = 86 Hz). IR: ν_{B-H} = 2528 cm^{-1}.

Collection and Reduction of X-ray Data. Crystals of **2**, dimensions 0.4 × 0.3 × 0.1 mm, and **3**, dimensions 0.3 × 0.3 × 0.1 mm, from the preparations above were selected and mounted on glass fibers. Data were collected at ambient temperatures on an Enraf-Nonius CAD4 computer controlled diffractometer with graphite-monochromatized Mo Kα radiation. Cell constants were determined by a least-squares fit to the centered angular coordinates of 24 intense reflections with 2θ values between 16 and 37°. An empirical absorption correction based on six ψ scans was applied. The intensities of three standard reflections remeasured every 120 min showed no decay. Crystallographic data for **2** and **3** are summarized in Table SI (supplementary material) and Table I.

Structure Solution and Refinement. The structures of **2** and **3** were solved by a combination of Patterson and direct methods.[28] For both structures, systematic absences indicated the space group $P2_1$ or $P2_1/m$. For **2**, refinement in the centrosymmetric setting was straightfoward. Attempts to refine **3** in the noncentrosymmetric space group $P2_1$ indicated a disorder of the Me and Br positions with large correlations between the positions related by the mirror in the centric space group (the occupancy of Br(2) in both positions refined to ~0.5). The centric space group $P2_1/m$ was therefore also chosen for **3** with a disorder of the Me and one Br across the mirror plane.

(28) SHELX-86: Sheldrick, G. M. In *Crystallographic Computing 3*; Sheldrick, G. M., Kruger, C., Goddard, R., Eds.; Oxford University Press: Oxford, U.K., 1985.

In the case of **2**, hydrogen atoms were included at their calculated positions (C-H = 0.95 Å) and were not refined. Hydrogen atoms were not included for **3**. The final difference Fourier map for **3** showed no peaks greater than 0.5 e/Å^3 except for several peaks between 0.5 and 1.9 e/Å^3 within 1 Å of the platinum. The final difference Fourier map for **2** showed several noise peaks as high as 5 e/Å^3 within 1 Å of the platinum. This may be due to a stacking disorder as observed in the wide mosaic for **2**. Several crystals were examined, and all showed high mosaic spread along *b*. Two complete data sets on two crystals were collected. The results for one were marginally better, and this is the set reported. Final positional parameters and bond distances and angles are listed in Tables II-V. Anisotropic thermal parameters for non-hydrogen atoms of **2** and **3** are given in Tables SII and SIII, positional and thermal parameters for the hydrogen atoms of **2** are listed in Table SIV, and observed and calculated structure factors are listed in Tables SVI and SVII (all supplementary material).

Acknowledgment. The support of this work by the Division of Chemical Sciences, Office of Basic Energy Sciences, Office of Energy Research, U.S. Department of Energy (Contract DE-FG02-88ER13880), and ARCO Chemical Co. is gratefully acknowledged. We thank Dr. Charles L. Barnes for assistance with the crystal structure determinations.

Supplementary Material Available: Crystal data collection and reduction parameters for **2** and **3** (Table SI), anisotropic thermal parameters for non-hydrogen atoms of **2** and **3** (Tables SII and SIII), positional and thermal parameters for the hydrogen atoms of **2** (Table SIV), and least-squares planes for the C_5 ring of **2** (Table SV) (5 pages); observed and calculated structure factors for **2** and **3** (Tables SVI and SVII) (10 pages). Ordering information is given on any current masthead page.

Contribution from the Department of Chemistry, The University of Alberta, Edmonton, Alberta, Canada T6G 2G2

Dithiophosphinate-Bridged Ruthenium(I) and Ruthenium(II) Complexes. Structure of $[Ru_2(CO)_4(\mu\text{-}S_2PMe_2)_2(PPh_3)_2]\cdot{}^1/_2CH_2Cl_2$

Robert W. Hilts and Martin Cowie*

Received February 9, 1990

Replacement of the bridging acetate groups in $[Ru_2(CO)_4(\mu\text{-}O_2CMe)_2(PR'_2R'')_2]$ (R', R'' = Ph, Me) by the dithiophosphinate anions $R_2PS_2^-$ (R = Me, Ph) yields a new class of dithiophosphinate-bridged Ru(I) complexes, $[Ru_2(CO)_4(\mu\text{-}S_2PR_2)_2(PR'_2R'')_2]$. Although the Ru-Ru bond in these species can be reversibly protonated, it does not react with $[Au(PPh_3)][BF_4]$, diazomethane, or dimethyl acetylenedicarboxylate. Reaction of the related acetate-bridged species $[Ru_2(CO)_4(\mu\text{-}O_2CMe)_2(NCMe)_2]$ with NaS_2PMe_2 does not yield the expected dithiophosphinate-bridged product but instead gives the mononuclear species $[Ru(CO)_2(\eta^2\text{-}S_2PMe_2)_2]$ along with Na_2S, NaO_2CMe, MeCN, and $Me_2P(S)P(S)Me_2$. An X-ray structure determination of $[Ru_2(CO)_4(\mu\text{-}S_2PMe_2)_2(PPh_3)_2]\cdot{}^1/_2CH_2Cl_2$ confirms the dithiophosphinate-bridged formulation and shows a long Ru-Ru separation of 2.9000 (6) Å and a twisting about the metal-metal axis by ca. 39°. This compound crystallizes in the monoclinic space group $P2_1/c$ with cell parameters a = 15.182 (3) Å, b = 18.230 (4) Å, c = 18.082 (4) Å, β = 94.23 (2)°, and Z = 4. Refinement has converged at R = 0.054 and R_w = 0.082 on the basis of 5928 unique reflections and 365 parameters varied.

Introduction

Dialkyl- and diaryldithiophosphinate anions, $R_2PS_2^-$, have proven to be versatile ligands that can bind in either a unidentate,[1-10] chelating,[1-22] or bridging[23-25] fashion to a wide range of transition metals. Of these binding modes, the chelating one is the most common, while complexes containing bridging $R_2PS_2^-$

(1) Cole-Hamilton, D. J.; Stephenson, T. A. *J. Chem. Soc., Dalton Trans.* **1974**, 739.
(2) Robertson, D. R.; Stephenson, T. A. *J. Organomet. Chem.* **1976**, *107*, C46.
(3) Faraone, F.; Marsala, V. *Inorg. Chim. Acta* **1976**, *17*, 217.
(4) Cole-Hamilton, D. J.; Stephenson, T. A. *J. Chem. Soc., Dalton Trans.* **1976**, 2396.
(5) Alison, J. M. C.; Gould, R. O.; Stephenson, T. A. *J. Chem. Soc. A* **1971**, 3690.
(6) Faithful, B. L.; Stephenson, T. A. *J. Chem. Soc. A* **1970**, 1504.
(7) Alison, J. M. C.; Fackler, J. P., Jr.; Fraser, A. J. F.; Gould, R. O.; Lin, I. J. B.; Stephenson, T. A.; Thompson, L. D. *Inorg. Chem.* **1982**, *21*, 2397.
(8) Colton, R.; Stephenson, T. A. *Polyhedron* **1984**, *3*, 231.
(9) Cornock, M. C.; Stephenson, T. A. *J. Chem. Soc., Dalton Trans.* **1977**, 501.
(10) Faraone, F.; Piraino, P. *Inorg. Chim. Acta* **1976**, *16*, 89.
(11) Cole-Hamilton, D. J.; Owen, J. D. *J. Chem. Soc., Dalton Trans.* **1974**, 1867.
(12) Appel, D. M.; Boyd, A. S. F.; Robertson, I. W.; Roundhill, D. M.; Stephenson, T. A. *Inorg. Chem.* **1982**, *21*, 449.
(13) Gogoi, P. K.; Mukherjee, R. N.; Shankar, S. *Polyhedron* **1985**, *4*, 1717.
(14) Cole-Hamilton, D. J.; Robertson, D. R.; Stephenson, T. A. *J. Chem. Soc., Dalton Trans.* **1975**, 1260.
(15) Sime, W. J.; Stephenson, T. A. *J. Chem. Soc., Dalton Trans.* **1978**, 1647.
(16) Byers, W.; Cavell, R. G.; Day, E. D. *Inorg. Chem.* **1971**, *10*, 2710.
(17) Byers, W.; Cavell, R. G.; Day, E. D.; Watkins, P. M. *Inorg. Chem.* **1971**, *10*, 2716.
(18) Kuchen, W.; Judat, A. *Chem. Ber.* **1967**, *100*, 991.
(19) Cole-Hamilton, D. J.; Stephenson, T. A. *J. Chem. Soc., Dalton Trans.* **1974**, 1818.
(20) Cornock, M. C.; Gould, R. O.; Jones, C. L.; Stephenson, T. A. *J. Chem. Soc., Dalton Trans.* **1977**, 1307.
(21) Lindner, E.; Matejcek, K.-M. *J. Organomet. Chem.* **1972**, *34*, 195.

0020-1669/90/1329-3349$02.50/0

groups are quite rare. For ruthenium, only complexes involving Ru(II) or Ru(III), having chelating or unidentate dithiophosphinate groups have been reported,[1,2,11,14,15] and, in fact, it appears that throughout the platinum group metals there are *no* examples involving this ligand in a bridging mode.

Our interest in developing the chemistry of binuclear, anion-bridged Ru(I) complexes[26] and the paucity of the bridging mode involving the $R_2PS_2^-$ ligand prompted us to explore the possibility of generating an unusual series of binuclear dithiophosphinate-bridged complexes of Ru(I). The results of this study are reported herein.

Experimental Section

General Considerations. All compounds were handled under dry nitrogen gas at ambient temperatures by using Schlenk techniques. Solvents were distilled and dried by using the appropriate desiccants immediately before use. The compounds $[Ru_2(CO)_4(\mu\text{-}O_2CMe)_2(NCMe)_2]$ (**1**),[27] $[Ru_2(CO)_4(\mu\text{-}O_2CMe)_2(PPh_3)_2]$ (**2**),[27] $Na[S_2PMe_2]$,[16] and $NH_4[S_2PPh_2]$[16] were prepared as previously reported. Trimethylphosphine (PMe_3), triphenylphosphine (PPh_3), dimethylphenylphosphine (PMe_2Ph), methyldiphenylphosphine (PPh_2Me), tricyclohexylphosphine (PCy_3), sodium hydride (NaH, 60% emulsion in oil), dimethyl acetylenedicarboxylate (DMA), and tetrafluoroboric acid diethyl etherate ($HBF_4{\cdot}Et_2O$) were purchased from Aldrich Chemicals Inc. and were used without further purification. Diazomethane was prepared by use of the Aldrich DIAZALD kit. Microanalyses were carried out within the department. Infrared spectra were run on either a Nicolet 7199 Fourier transform interferometer or a Perkin-Elmer 883 spectrophotometer as Nujol mulls on KBr disks. The $^{31}P\{^1H\}$ NMR spectra were recorded on either a Bruker AM-400 Fourier transform NMR spectrometer operating at 161.98 MHz or a Bruker AM-200 instrument operating at 81.0 MHz, and ^1H and $^{13}C\{^1H\}$ NMR spectra were recorded at 300.1 and 75.5 MHz, respectively on a Bruker AM-300 spectrometer. All $^1H\{^{31}P\}$ heteronuclear decoupling experiments were performed on the Bruker AM-400 instrument. The ^{31}P chemical shifts are reported in parts per million (ppm) relative to 85% H_3PO_4 whereas ^{13}C and ^1H chemical shifts are with respect to $Si(CH_3)_4$.

Preparation of the Compounds. (1) $[Ru_2(CO)_4(\mu\text{-}O_2CMe)_2(PR_2R')_2]$ (R = Ph, R' = Me (3); R = Me, R' = Ph (4); R = R' = Me (5); R = R' = Cy (6)). These compounds were prepared by using essentially the same procedure as that reported for the synthesis of $[Ru_2(CO)_4(\mu\text{-}O_2CMe)_2(PPh_3)_2]$ (**2**).[27] Typically, 2 molar equiv of the appropriate phosphine was added directly to a stirred solution of $[Ru_2(CO)_4(\mu\text{-}O_2CMe)_2(NCMe)_2]$ (**1**) in 10 mL of THF, causing an immediate change in color from orange to yellow. After 2 h of stirring, the solvent was removed in vacuo and the resultant yellow residue was kept under vacuum for several hours. Pertinent information on each compound is given below.

$[Ru_2(CO)_4(\mu\text{-}O_2CMe)_2(PPh_2Me)_2]$ (3). Yellow crystalline solid. Yield: 87%. Recrystallized from THF/Et_2O at 23 °C. Anal. Calcd for $C_{34}H_{32}O_8P_2Ru_2$: C, 49.04; H, 3.87. Found: C, 49.10; H, 3.85.

$[Ru_2(CO)_4(\mu\text{-}O_2CMe)_2(PMe_2Ph)_2]$ (4). Yellow crystalline solid. Yield: 83%. Recrystallized from hexane at 23 °C. Anal. Calcd for $C_{24}H_{28}O_8P_2Ru_2$: C, 40.68; H, 3.98. Found: C, 40.68; H, 4.01.

$[Ru_2(CO)_4(\mu\text{-}O_2CMe)_2(PMe_3)_2]$ (5). Yellow solid. Yield: 94%. Recrystallized from THF/Et_2O at 23 °C. Anal. Calcd for $C_{14}H_{24}O_8P_2Ru_2$: C, 28.77; H, 4.14. Found: C, 28.73; H, 3.95.

$[Ru_2(CO)_4(\mu\text{-}O_2CMe)_2(PCy_3)_2]$ (6). Yellow solid. Precipitated from THF with hexane. Anal. Calcd for $C_{44}H_{72}O_8P_2Ru_2$: C, 53.21; H, 7.31. Found: C, 53.96; H, 7.57.

(2) $[Ru_2(CO)_4(\mu\text{-}S_2PR_2)_2(PR'_2R'')_2]$ (R = Me, R' = R'' = Ph (7); R = Me, R' = Ph, R'' = Me (8); R = Me, R' = Me, R'' = Ph (9); R = R' = R'' = Me (10); R = R' = R'' = Ph (11)). All of the dithiophosphinate-bridged Ru(I) dimers were prepared by using procedures similar to that described as follows for complex **7**. Sodium dimethyldithiophosphinate (0.077 g, 0.522 mmol) was added as a solid to a stirred solution of $[Ru_2(CO)_4(\mu\text{-}O_2CMe)_2(PPh_3)_2]$ (**2**) (0.250 g, 0.261 mmol) in 20 mL of THF. Within 5 h, the color of the solution had changed from yellow to orange and a bright yellow-orange solid had precipitated. After 15 h of stirring, the solvent was removed under vacuum, leaving an orange-yellow residue, which was extracted with 25 mL of CH_2Cl_2. The resulting cloudy yellow solution was filtered to remove precipitated sodium acetate, the clear filtrate transferred to a second flask, and the solvent again removed under vacuum. Dissolution of the remaining orange solid in 1 mL of THF and the addition of 20 mL of Et_2O caused the immediate precipitation of a yellow-orange solid, which was recrystallized from CH_2Cl_2/Et_2O to give $[Ru_2(CO)_4(\mu\text{-}S_2PMe_2)_2(PPh_3)_2]{\cdot}^1/_2CH_2Cl_2$ (**7**) (0.221 g, 0.203 mmol) as orange crystals. Yield: 81%. Anal. Calcd for $C_{44.5}H_{43}ClO_4P_4Ru_2S_4$: C, 47.23; H, 3.83; Cl, 3.83. Found: C, 47.11; H, 3.44; Cl, 2.75.

The crystallization conditions, colors, and yields obtained for the other members of this class of compounds are given below along with their microanalytical results. All spectroscopic data for the dithiophosphinate-bridged species are provided in Table I.

$[Ru_2(CO)_4(\mu\text{-}S_2PMe_2)_2(PPh_2Me)_2]$ (8). Orange-yellow crystalline solid. Recrystallized from CH_2Cl_2/hexane at 23 °C. Yield: 93%. Anal. Calcd for $C_{34}H_{38}O_4P_4Ru_2S_4$ C, 42.32; H, 3.97. Found: C, 42.07; H, 3.79.

$[Ru_2(CO)_4(\mu\text{-}S_2PMe_2)_2(PMe_2Ph)_2]$ (9). Orange solid. Recrystallized from hexane at −18 °C. Yield: 75%. Anal. Calcd for $C_{24}H_{34}O_4P_4Ru_2S_4$: C, 34.28; H, 4.08. Found: C, 34.40; H, 4.11.

$[Ru_2(CO)_4(\mu\text{-}S_2PMe_2)_2(PMe_3)_2]$ (10). Orange-yellow solid. Characterized by $^{31}P\{^1H\}$ and $^{13}C\{^1H\}$ NMR spectroscopy.

$[Ru_2(CO)_4(\mu\text{-}S_2PPh_2)_2(PPh_3)_2]$ (11). Orange-yellow solid. Precipitated from CH_2Cl_2 with hexane. Yield: 94%. Anal. Calcd for $C_{64}H_{50}O_4P_4Ru_2S_4$: C, 57.48; H, 3.77. Found: C, 57.16; H, 4.10.

(3) $[Ru_2(CO)_4(\mu\text{-}H)(\mu\text{-}S_2PMe_2)_2(PPh_2R)_2][BF_4]$ [R = Ph (12); R = Me (13)). Both of the hydrido-bridged Ru(II) dimers were prepared by using the procedure described below for the synthesis of complex **12**. Tetrafluoroboric acid diethyl etherate (0.015 g, 0.08 mmol) was added to a stirred solution of $[Ru_2(CO)_4(\mu\text{-}S_2PMe_2)_2(PPh_3)_2]$ (**7**) (0.088 g, 0.081 mmol) in 20 mL of CH_2Cl_2, resulting in an immediate color change from orange to yellow. After 1 h of stirring, the solvent was removed under vacuum, leaving a yellow tar. This residue was dissolved in 2 mL of THF, and 20 mL of Et_2O was added, causing the immediate precipitation of $[Ru_2(CO)_4(\mu\text{-}H)(\mu\text{-}S_2PMe_2)_2(PPh_3)_2][BF_4]{\cdot}CH_2Cl_2$ (**12**) (0.07 g, 0.055 mmol) as a bright yellow solid. Yield: 69%. Anal. Calcd. for $C_{45}H_{45}BCl_2F_4O_4P_4Ru_2S_4$: C, 42.83; H, 3.59. Found: C, 41.97; H, 3.51.

$[Ru_2(CO)_4(\mu\text{-}H)(\mu\text{-}S_2PMe_2)_2(PPh_2Me)_2][BF_4]$ (13). Orange-yellow solid. Yield: 83%. Anal. Calcd for $C_{34}H_{39}BF_4O_4P_4Ru_2S_4$: C, 38.79; H, 3.73. Found: C, 38.05; H, 3.85.

(4) Attempted Reaction of $[Au(PPh_3)][BF_4]$ with $[Ru_2(CO)_4(\mu\text{-}S_2PMe_2)_2(PPh_3)_2]$ (7). One molar equivalent of $[Au(PPh_3)][BF_4]$ (prepared in acetone from $AuPPh_3Cl$ and $AgBF_4$) in 10 mL of THF was syringed into a solution of $[Ru_2(CO)_4(\mu\text{-}S_2PMe_2)_2(PPh_3)_2]$ (**7**) in 20 mL of THF. Stirring was continued for 24 h with no apparent change. $^{31}P\{^1H\}$ NMR and IR spectroscopy showed only starting material. Similarly, compound **8** also failed to react with $[Au(PPh_3)][BF_4]$.

(5) Reaction of Sodium Hydride with $[Ru_2(CO)_4(\mu\text{-}H)(\mu\text{-}S_2PMe_2)_2(PPh_3)_2][BF_4]$ (12). Sodium hydride (0.030 g, 60% emulsion in oil, 0.75 mmol) and $[Ru_2(CO)_4(\mu\text{-}H)(\mu\text{-}S_2PMe_2)_2(PPh_3)_2][BF_4]{\cdot}CH_2Cl_2$ (**12**·CH_2Cl_2) (0.100 g, 0.079 mmol) were stirred together in 10 mL of THF for 1 h. During this time gas was evolved and the solution gradually changed color from yellow to yellow-orange. The unreacted sodium hydride was allowed to settle, and the clear orange-yellow supernatant was transferred to a second vessel from which the solvent was removed under vacuum. The $^{31}P\{^1H\}$ NMR spectrum of the orange-yellow residue in THF contained only $[Ru_2(CO)_4(\mu\text{-}S_2PMe_2)_2(PPh_3)_2]$ (**7**).

(6) Reaction of $[Ru_2(CO)_4(\mu\text{-}O_2CMe)_2(NCMe)_2]$ (1) with NaS_2PMe_2. Sodium dimethyldithiophosphinate (0.173 g, 1.17 mmol) was added directly to a stirred orange solution of $[Ru_2(CO)_4(\mu\text{-}O_2CMe)_2(NCMe)_2]$ (**1**) (0.100 g, 0.195 mmol) in 10 mL of THF, causing the solution to immediately become red. The mixture was stirred for 14 h and then taken to dryness under vacuum. The orange-red residue was dissolved in 20 mL of CH_2Cl_2 and filtered to remove precipitated sodium acetate. The clear orange supernatant was transferred to a second flask and the solvent was removed under vacuum. Orange-brown crystals of $[Ru(CO)_2(\eta^2\text{-}S_2PMe_2)_2]$ (**14**) (0.097 g, 0.238 mmol) were grown from toluene/Et_2O at 23 °C. The supernatant above the crystals of **14** was found to contain a second phosphorus-containing species (δ 35.21, singlet), tentatively identified as $Me_2P(S)P(S)Me_2$.[28-30] Yield for $[Ru(CO)_2$-

(22) Lambert, E. L.; Manuel, T. A. *Inorg. Chem.* **1966**, *5*, 1287.
(23) (a) Calligaris, M.; Nardin, G.; Ripamonti, A. *J. Chem. Soc., Chem. Commun.* **1968**, 1014. (b) Calligaris, M.; Nardin, G.; Ripamonti, A. *J. Chem. Soc. A* **1970**, 714.
(24) Kuchen, W.; Mayatepek, H. *Chem. Ber.* **1968**, *101*, 3454.
(25) Burk, J. H.; Burlitch, J. M.; Lemley, J. T.; Whitwell, G. E., II. *Inorg. Chem.* **1983**, *22*, 1306.
(26) Cowie, M.; Sherlock, S. J.; Singleton, E.; de V. Steyn, M. M. *J. Organomet. Chem.* **1989**, *361*, 353.
(27) Crooks, G. R.; Gamlen, G.; Johnson, B. F. G.; Lewis, J.; Williams, I. G. *J. Chem. Soc. A* **1969**, 2761.
(28) Harris, R. K.; Hayter, R. G. *Can. J. Chem.* **1964**, *42*, 2282.
(29) Mavel, G. Studies of Phosphorus Compounds Using the Magnetic Resonance Spectra of Nuclei Other than Phosphorus-31. In *Progress in NMR Spectroscopy*; Emsley, J. W., Feeney, J., Sutcliffe, L. H., Eds.; Pergamon Press: Oxford, England, 1966; Vol. 1, Chapter 4, pp 252–373.

Table I. Spectral Data[a]

	IR, cm^{-1} [b]		NMR		
	ν_{CO}	ν_{PS_2}	$\delta(^{31}P\{^1H\})$[c]	$\delta(^1H)$[d]	$\delta(^{13}C\{^1H\})$[d]
$[Ru_2(CO)_4(\mu\text{-}S_2PMe_2)_2(PPh_3)_2]$ (**7**)[e]	2019 (vs), 1984 (vs), 1932 (vs), 1896 (w)	549 (st), 524 (m)	S_2PMe_2: 97.51 (t); PPh_3: 14.07 (t); $^3J_{PP}$ = 57 Hz	S_2PMe_2: 1.89 (d), 2.26 (d); $^2J_{PH}$ = 12, 13 Hz	S_2PMe_2: 30.45 (d), 30.83 (d); $^1J_{PC}$ = 51, 51 Hz; CO: 203.49 (s)
$[Ru_2(CO)_4(\mu\text{-}S_2PMe_2)_2(PPh_2Me)_2]$ (**8**)[f]	2013 (vs), 1967 (st), 1938 (vs), 1921 (m)	554 (m), 511 (m)	S_2PMe_2: 98.53 (t); PPh_2Me: 1.23 (t); $^3J_{PP}$ = 61 Hz	S_2PMe_2: 1.88 (d), 2.13 (d); $^2J_{PH}$ = 12, 13 Hz; PPh_2Me: 2.06 (vt); $^1/_2[^2J_{PH} + {}^5J_{PH}]$ = 4 Hz	S_2PMe_2: 31.23 (d), 30.27 (d); $^1J_{PC}$ = 51, 51 Hz; PPh_2Me: 14.80 (vt); $^1/_2[^1J_{PC} + {}^4J_{PC}]$ = 12 Hz; CO: 203.49 (s)
$[Ru_2(CO)_4(\mu\text{-}S_2PMe_2)_2(PPhMe_2)_2]$ (**9**)[f]	2010 (vs), 1966 (m), 1936 (vs), 1918 (sh)	550 (m)	S_2PMe_2: 77.93 (t); $PPhMe_2$: −10.00 (t); $^3J_{PP}$ = 68 Hz	S_2PMe_2: 1.92 (d), 2.13 (d); $^2J_{PH}$ = 12, 13 Hz; $PPhMe_2$: 1.79 (vt); $^1/_2[^2J_{PH} + {}^5J_{PH}]$ = 4 Hz	S_2PMe_2: 31.53 (d), 30.53 (d); $^1J_{PC}$ = 51, 51 Hz; $PPhMe_2$: 14.55 (vt); $^1/_2[^1J_{PC} + {}^4J_{PC}]$ = 13 Hz; CO: 204.04
$[Ru_2(CO)_4(\mu\text{-}S_2PMe_2)_2(PMe_3)_2]$ (**10**)[f]	2016 (vs), 1969 (m), 1936 (s), 1890 (w)	[g]	S_2PMe_2: 99.38 (t); PMe_3: −19.12 (t); $^3J_{PP}$ = 75 Hz		$SPMe_2$: 31.57 (d), 30.74 (d); $^1J_{PC}$ = 51, 51 Hz; PMe_3: 16.75 (vt); $^1/_2[^1J_{PC} + {}^4J_{PC}]$ = 13 Hz; CO: 204.99 (s)
$[Ru_2(CO)_4(\mu\text{-}S_2PPh_2)_2(PPh_3)_2]$ (**11**)[e]	2016 (vs), 1974 (st), 1943 (st), 1926 (m)	550 (m), 519 (m)	S_2PPh_2: 100.81 (t); PPh_3: 15.82 (t); $^3J_{PP}$ = 58 Hz		
$[Ru_2(CO)_4(\mu\text{-}H)(\mu\text{-}S_2PMe_2)_2(PPh_3)_2][BF_4]$ (**12**)[f,h]	2054 (vs), 1988 (st), 1982 (st)	562 (m), 525 (m)	S_2PMe_2: 89.33 (t); PPh_3: 32.01 (t); $^3J_{PP}$ = 26 Hz	S_2PMe_2: 2.23 (d), 2.02 (d); $^2J_{PH}$ = 13, 12 Hz; μ-H: −16.84 (tt); $^3J_{S_2PMe_2-H}$ = 18 Hz, $^2J_{PPh_3-H}$ = 32 Hz	S_2PMe_2: 29.73 (d), 28.76 (d); $^1J_{PC}$ = 54, 54 Hz; CO: 191.59 (s)
$[Ru_2(CO)_4(\mu\text{-}H)(\mu\text{-}S_2PMe_2)_2(PPh_2Me)_2][BF_4]$ (**13**)[f,i]	2053 (vs), 2004 (vs), 1924 (st)	559 (st), 501 (s)	S_2PMe_2: 87.23 (t); PPh_2Me: 18.94 (t); $^3J_{PP}$ = 28 Hz	S_2PMe_2: 2.25 (d), 2.11 (d); $^2J_{PH}$ = 13, 12 Hz; PPh_2Me: 2.31 (vt); $^1/_2[^2J_{PH} + {}^5J_{PH}]$ = 5 Hz; μ-H: −16.10 (tt); $^3J_{S_2PMe_2-H}$ = 19 Hz, $^2J_{PPh_3-H}$ = 30 Hz	S_2PMe_2: 29.13 (d), 28.59 (d); $^1J_{PC}$ = 54, 54 Hz; PPh_2Me: 16.65 (vt); $^1/_2[^1J_{PC} + {}^4J_{PC}]$ = 18 Hz; CO: 191.65 (vt); $^1/_2[^2J_{PC} + {}^3J_{PC}]$ = 5 Hz
$[Ru(CO)_2(\eta^2\text{-}S_2PMe_2)_2]$ (**14**)[f]	2033 (st), 1970 (st)	585 (m), 563 (m)	S_2PMe_2: 92.96 (s)	S_2PMe_2: 2.07 (d), 1.95 (d); $^2J_{PH}$ = 13, 13 Hz	S_2PMe_2: 31.65 (d), 29.30 (d); $^1J_{PC}$ = 42, 45 Hz; CO: 194.69, 194.67
NaS_2PMe_2[j]		602 (m), 560 (m)	S_2PMe_2: 54.33 (s)	S_2PMe_2: 1.93 (d); $^2J_{PH}$ = 13 Hz	S_2PMe_2: 33.56 (d); $^1J_{PC}$ = 56 Hz
$NH_4S_2PPh_2$[j]		612 (m), 560 (m)	S_2PMe_2: 62.02 (s)		

[a] Abbreviations used: vs, very strong; st, strong; bs, broad and strong; m, medium; w, weak; sh, shoulder; s, singlet; d, doublet; t, triplet; tt, triplet of triplets; vt, virtual triplet. [b] All IR spectra were obtained as Nujol mulls. [c] Vs 85% H_3PO_4. [d] Vs TMS. [e] CD_2Cl_2 was used as the NMR solvent. [f] $CDCl_3$ was used as the NMR solvent. [g] Not observed. [h] $\nu_{BF_4^-}$: 1067 cm^{-1}. [i] $\nu_{BF_4^-}$: 1058 cm^{-1}. [j] CD_3OD was used as the NMR solvent.

$(\eta^2\text{-}S_2PMe_2)_2]$: 61% (based upon complete conversion of $[Ru_2(CO)_4(\mu\text{-}O_2CMe)_2(NCMe)_2]$ (**1**)). Anal. for $[Ru(CO)_2(\eta^2\text{-}S_2PMe_2)_2]$ (**14**). Calcd for $C_6H_{12}O_2P_2RuS_4$: C, 17.69; H, 2.97. Found: C, 17.79; H, 2.60.

(7) Attempted Reactions of CH_2N_2 and Dimethyl Acetylenedicarboxylate with Compounds 7 and 8. Tetrahydrofuran solutions of $[Ru_2(CO)_4(\mu\text{-}S_2PMe_2)_2(PPh_3)_2]$ (**7**) and $[Ru_2(CO)_4(\mu\text{-}S_2PMe_2)_2(PPh_2Me)_2]$ (**8**) were charged with 1 molar equiv of either diazomethane or dimethyl acetylenedicarboxylate and stirred for 24 h in sealed flasks. $^{31}P\{^1H\}$ NMR spectroscopy performed upon the reaction mixtures indicated that the only phosphorus-containing species present were the starting Ru dimers, **7** and **8**. Increasing the reaction time and tripling the amount of added CH_2N_2 or dimethyl acetylenedicarboxylate succeeded only in producing several unknown decomposition products.

X-ray Data Collection. Yellow-orange crystals of $[Ru_2(CO)_4(\mu\text{-}S_2PMe_2)_2(PPh_3)_2]\cdot{}^1/_2CH_2Cl_2$ (**7**) were obtained by slow diffusion of Et_2O into a concentrated CH_2Cl_2 solution of the compound. Data were collected on an Enraf-Nonius CAD4 diffractometer using graphite-monochromated Mo Kα X-radiation. A suitable crystal was mounted on a glass fiber. Unit cell parameters were obtained from a least-squares refinement of the setting angles of 24 reflections in the range $22.0° \le 2\theta \le 26.0°$. The monoclinic diffraction symmetry and the systematic absences ($h0l$, l = odd; $0k0$, k = odd) were consistent with the space group $P2_1/c$. Intensity data were collected at 22 °C with the $\theta/2\theta$ scan technique to $2\theta = 50.0°$. Backgrounds for the peaks were measured by extending the scan 25% on either side of the calculated range. The three standard reflections, collected every 60 min of exposure, showed no significant decay in intensity during data collection, and thus no correction was applied. The crystallographic data are summarized in Table II, and the details of intensity collection are given in the supplementary material. In total, 8646 unique reflections were measured and reduced in the usual manner by using $p = 0.04$ to down-weight intense reflections;[31] of these, 5928 were observed and were used in subsequent refinements. The method of Walker and Stuart was used to correct data for absorption effects.[32]

Table II. Crystallographic Data for $[Ru_2(CO)_4(\mu\text{-}S_2PMe_2)_2(PPh_3)_2]\cdot{}^1/_2CH_2Cl_2$ (**7**)

$C_{44}H_{42}O_4P_4Ru_2S_4\cdot{}^1/_2CH_2Cl_2$	fw: 1131.59
a = 15.182 (3) Å	space group: $P2_1/c$
b = 18.230 (4) Å	T = 22 °C
c = 18.082 (4) Å	λ = 0.71073 Å
β = 94.23 (2)°	ρ(calcd) = 1.514 g·cm^{-3}
μ = 9.730 cm^{-1}	transm coeff = 0.783–1.138
V = 4990.9 Å^3	R = 0.054
Z = 4	R_w = 0.082

Structure Solution and Refinement. The Ru positions were obtained by Patterson techniques, while the other atoms were located by the usual sequence of least-squares and difference Fourier calculations. The phenyl

(30) Crutchfield, M. M.; Dungan, C. H.; Letcher, J. H.; Mark, V.; Van Wazer, J. R. *Topics in Phosphorus Chemistry, Volume 5: ^{31}P Nuclear Magnetic Resonance*; Interscience Publishers: New York, 1967.

(31) Doedens, R. J.; Ibers, J. A. *Inorg. Chem.* **1967**, *6*, 204.

(32) (a) Stuart, D.; Walker, N. *Acta Crystallogr., Sect. A* **1983**, *39*, 1581. (b) Programs used for solution and refinement of the structure were those of the Enraf-Nonius Structure Determination Package by B. A. Frenz, in addition to local programs by R. G. Ball.

Table III. Positional and Thermal Parameters for the Inner-Core Atoms of $[Ru_2(CO)_4(\mu\text{-}S_2PMe_2)_2(PPh_3)_2]\cdot{}^1/_2CH_2Cl_2$ (**7**)[a]

atom	x	y	z	B, Å²[b]
Ru(1)	0.22737 (4)	0.18055 (4)	−0.22405 (4)	1.94 (1)
Ru(2)	0.28926 (4)	0.03006 (4)	−0.22427 (4)	1.90 (1)
S(1)	0.1361 (2)	0.1652 (1)	−0.3430 (1)	3.28 (5)
S(2)	0.1418 (2)	−0.0121 (1)	−0.2772 (1)	2.94 (5)
S(3)	0.3587 (2)	0.2218 (1)	−0.2867 (1)	2.69 (5)
S(4)	0.3489 (2)	0.0429 (2)	−0.3482 (1)	3.22 (5)
P(1)	0.0999 (2)	0.0596 (2)	−0.3559 (2)	4.05 (6)
P(2)	0.3821 (2)	0.1481 (1)	−0.3648 (1)	3.07 (5)
P(3)	0.1744 (2)	0.3051 (1)	−0.2184 (1)	2.34 (5)
P(4)	0.3334 (1)	−0.0964 (1)	−0.2210 (1)	2.07 (4)
O(1)	0.3329 (6)	0.1958 (4)	−0.0791 (4)	5.5 (2)
O(2)	0.0731 (5)	0.1220 (4)	−0.1466 (5)	5.9 (2)
O(3)	0.2365 (6)	0.0255 (4)	−0.0680 (4)	5.3 (2)
O(4)	0.4673 (5)	0.0868 (4)	−0.1630 (5)	4.9 (2)
C(1)	0.2919 (6)	0.1889 (5)	−0.1356 (5)	2.8 (2)
C(2)	0.1310 (6)	0.1429 (5)	−0.1766 (5)	3.2 (2)
C(3)	0.2528 (6)	0.0262 (5)	−0.1295 (5)	3.0 (2)
C(4)	0.4004 (6)	0.0665 (6)	−0.1870 (5)	3.0 (2)
C(5)	−0.0133 (9)	0.0517 (8)	−0.369 (1)	8.8 (4)
C(6)	0.132 (1)	0.0287 (7)	−0.4435 (7)	6.7 (4)
C(7)	0.331 (1)	0.1763 (6)	−0.4524 (6)	5.8 (3)
C(8)	0.4969 (8)	0.1546 (7)	−0.3766 (8)	6.3 (3)

[a] Phenyl carbons and the solvent molecule are given in the supplementary material. [b] Anisotropically refined atoms are given in the form of the isotropic equivalent displacement parameter defined as $(4/3)[a^2\beta(1,1) + b^2\beta(2,2) + c^2\beta(3,3) + ab(\cos\gamma)\beta(1,2) + ac(\cos\beta)\beta(1,3) + bc(\cos\alpha)\beta(2,3)]$.

Table IV. Intramolecular Bond Lengths (Å) for $[Ru_2(CO)_4(\mu\text{-}S_2PMe_2)_2(PPh_3)_2]\cdot{}^1/_2CH_2Cl_2$ (**7**)[a,b]

Ru(1)–Ru(2)	2.9000 (6)	S(2)–P(1)	2.001 (2)
Ru(1)–S(1)	2.486 (2)	S(3)–P(2)	2.000 (2)
Ru(1)–S(3)	2.482 (2)	S(4)–P(2)	2.010 (2)
Ru(1)–P(3)	2.414 (2)	P(1)–C(5)	1.722 (9)
Ru(1)–C(1)	1.820 (6)	P(1)–C(6)	1.782 (9)
Ru(1)–C(2)	1.881 (7)	P(2)–C(7)	1.788 (8)
Ru(2)–S(2)	2.491 (2)	P(2)–C(8)	1.775 (8)
Ru(2)–S(4)	2.489 (2)	O(1)–C(1)	1.163 (7)
Ru(2)–P(4)	2.402 (1)	O(2)–C(2)	1.132 (7)
Ru(2)–C(3)	1.841 (6)	O(3)–C(3)	1.157 (7)
Ru(2)–C(4)	1.891 (7)	O(4)–C(4)	1.135 (7)
S(1)–P(1)	2.012 (2)		

[a] Numbers in parentheses are estimated standard deviations in the least significant digits. [b] Bond lengths within the phenyl rings are given in the supplementary material.

carbon atoms of the triphenylphosphine ligands were refined isotropically. A molecule of cocrystallized CH_2Cl_2 was located and found to have half-occupancy. This was corroborated by chlorine analysis and ^1H NMR spectroscopy. Although all hydrogens within the complex were located, they were not refined but were placed in their idealized positions with C–H distances of 0.95 Å and the appropriate hybridization geometry of the attached carbon atom. Methylene chloride hydrogens were not included. Thermal parameters for the hydrogen atoms were fixed at 1.2 times the isotropic B of the attached carbon atom. Refinement of the structure was carried out by the full-matrix least-squares techniques using atomic scattering factors[33,34] and anomalous dispersion terms[35] taken from the usual sources. The structure converged to R = 0.054 and R_w = 0.082 with 365 parameters refined.

Results

The spectroscopic data for all of the compounds are presented in the Discussion and are tabulated in Table I. The structure determination for $[Ru_2(CO)_4(\mu\text{-}S_2PMe_2)_2(PPh_3)_2]\cdot{}^1/_2CH_2Cl_2$ is discussed below. The positional and isotropic thermal parameters for the most relevant, inner-core atoms of compound **7** are given in Table III, and the bond lengths and angles are collected in Tables IV and V, respectively. Additional information is available as supplementary material.

Table V. Intramolecular Angles (deg) for $[Ru_2(CO)_4(\mu\text{-}S_2PMe_2)_2(PPh_3)_2]\cdot{}^1/_2CH_2Cl_2$ (**7**)

(a) Bond Angles

Ru(2)–Ru(1)–S(1)	93.01 (4)	P(4)–Ru(2)–C(4)	95.1 (2)
Ru(2)–Ru(1)–S(3)	90.83 (4)	C(3)–Ru(2)–C(4)	90.2 (3)
Ru(2)–Ru(1)–P(3)	177.53 (4)	Ru(1)–S(1)–P(1)	109.75 (9)
Ru(2)–Ru(1)–C(1)	85.8 (2)	Ru(2)–S(2)–P(1)	107.52 (8)
Ru(2)–Ru(1)–C(2)	85.4 (2)	Ru(1)–S(3)–P(2)	108.01 (8)
S(1)–Ru(1)–S(3)	93.11 (6)	Ru(2)–S(4)–P(2)	109.63 (8)
S(1)–Ru(1)–P(3)	88.63 (5)	S(1)–P(1)–S(2)	118.2 (1)
S(1)–Ru(1)–C(1)	177.9 (2)	S(1)–P(1)–C(5)	111.0 (3)
S(1)–Ru(1)–C(2	87.3 (2)	S(1)–P(1)–C(6)	108.4 (3)
S(3)–Ru(1)–P(3)	90.92 (5)	S(2)–P(1)–C(5)	107.6 (3)
S(3)–Ru(1)–C(1)	88.8 (2)	S(2)–P(1)–C(6)	109.5 (3)
S(3)–Ru(1)–C(2)	176.1 (2)	C(5)–P(1)–C(6)	100.8 (5)
P(3)–Ru(1)–C(1)	92.5 (2)	S(3)–P(2)–S(4)	118.4 (1)
P(3)–Ru(1)–C(2)	92.9 (2)	S(3)–P(2)–C(7)	110.1 (3)
C(1)–Ru(1)–C(2)	91.0 (3)	S(3)–P(2)–C(8)	105.4 (3)
Ru(1)–Ru(2)–S(2)	90.58 (4)	S(4)–P(2)–C(7)	108.1 (3)
Ru(1)–Ru(2)–S(4)	92.97 (4)	S(4)–P(2)–C(8)	109.9 (3)
Ru(1)–Ru(2)–P(4)	176.84 (4)	C(7)–P(2)–C(8)	103.9 (5)
Ru(1)–Ru(2)–C(3)	85.1 (2)	Ru(1)–P(3)–C(11)	120.4 (2)
Ru(1)–Ru(2)–C(4)	87.1 (2)	Ru(1)–P(3)–C(21)	117.7 (2)
S(2)–Ru(2)–S(4)	93.42 (6)	Ru(1)–P(3)–C(31)	107.1 (2)
S(2)–Ru(2)–P(4)	87.40 (5)	Ru(2)–P(4)–C(41)	108.4 (2)
S(2)–Ru(2)–C(3)	91.3 (2)	Ru(2)–P(4)–C(51)	119.5 (2)
S(2)–Ru(2)–C(4)	177.1 (2)	Ru(2)–P(4)–C(61)	118.0 (2)
S(4)–Ru(2)–P(4)	89.59 (5)	Ru(1)–C(1)–O(1)	178.7 (5)
S(4)–Ru(2)–C(3)	175.0 (2)	Ru(1)–C(2)–O(2)	177.9 (6)
S(4)–Ru(2)–C(4)	85.1 (2)	Ru(2)–C(3)–O(3)	174.6 (6)
P(4)–Ru(2)–C(3)	92.5 (2)	Ru(2)–C(4)–O(4)	178.0 (6)

(b) Torsion Angles

C(1)–Ru(1)–Ru(2)–C(4)	−40.7 (4)
C(2)–Ru(1)–Ru(2)–C(3)	−41.5 (4)
S(1)–Ru(1)–Ru(2)–S(2)	−37.2 (1)
S(3)–Ru(1)–Ru(2)–S(4)	−36.9 (1)

Discussion

We have previously shown that the acetate-bridged complexes $[Ru_2(CO)_4(\mu\text{-}O_2CMe)_2(NCMe)_2]$ (**1**) and $[Ru_2(CO)_4(\mu\text{-}O_2CMe)_2(PPh_3)_2]$ (**2**) can serve as useful precursors to an unusual series of anion-bridged Ru(I) complexes, either by replacement of the acetate bridges by other anionic bridging groups, such as pyrazolate, mercaptothiazolinate, and oxypyridinate,[26] or by substitution of the labile acetonitrile ligands with neutral bidentate ligands, which also can act as bridging groups.[36] It seemed that the precursors mentioned above could also provide a route into chemistry involving the bridging dithiophosphinate ligand. As noted earlier, the bridging mode for this ligand is quite rare and, before this work, was apparently unknown with platinum group metals. This is presumably a function of the large bite (ca. 3.3 Å) of this ligand, which can cause strain within a bridged metal–metal-bonded system. The chelating mode for this group is generally favored because it involves the formation of stable four-membered rings that have large bite angles and hence, very little internal strain.[23] It was of interest to compare the structural differences between other relatively unstrained Ru–Ru-bonded systems and one involving the large dithiophosphinate groups, with the intention of determining whether any strain imposed by the latter in a bridging mode would result in weakening of the Ru–Ru bond and a concomitant increase in the reactivity of this moiety.

The target complexes $[Ru_2(CO)_4(\mu\text{-}S_2PR_2)_2(PR'_2R'')_2]$ (**7–11**) (R = Me, Ph; R′ = Me, Ph; R″ = Me, Ph) are readily prepared by treating the acetate-bridged precursors $[Ru_2(CO)_4(\mu\text{-}O_2CMe)_2(PR'_2R'')_2]$ (**2–5**) with 2 equiv of the sodium or ammonium salts of the appropriate dithiophosphinate anions. The NMR data for the acetate-bridged compounds **2–6** have been included in the supplementary material, since most of these data have apparently not been previously reported; their syntheses follow

(33) Davidson, E. F.; Simpson, W. T.; Stewart, R. F. *J. Chem. Phys.* **1965**, *42*, 3175.
(34) Cromer, D. T.; Waber, J. T. *International Tables for X-ray Crystallography*; Kynoch Press: Birmingham, England, 1974; Vol. IV, Table 2.2A.
(35) Cromer, D. T.; Liberman, D. *J. Chem. Phys.* **1970**, *53*, 1891.
(36) Cowie, M.; Sherlock, S. J.; Singleton, E.; de V. Steyn, M. M. *Organometallics* **1988**, *7*, 1663.

directly from the route reported for the preparation of $[Ru_2(CO)_4(\mu\text{-}O_2CMe)_2(PPh_3)_2]$ (**2**), which involves replacement of the labile acetonitrile groups in $[Ru_2(CO)_4(\mu\text{-}O_2CMe)_2(NCMe)_2]$ (**1**) by phosphine ligands.[27] We were unable to synthesize the dithiophosphinate-bridged complexes containing tricyclohexylphosphine ligands, starting from **6**, presumably owing to the large bulk of this phosphine. In addition we find that the osmium analogues, $[Os_2(CO)_4(\mu\text{-}O_2CMe)_2(PR'_2R'')_2]$, are inert to substitution of the bridging acetate groups, even in the presence of large excesses of the dithiophosphinate anion and at temperatures up to 260 °C. These findings are consistent with a previous study which showed that ruthenium complexes are much more reactive than their osmium analogues.[27]

The $^{31}P\{^1H\}$, $^{13}C\{^1H\}$, and ^1H NMR data for the dithiophosphinate-bridged Ru(I) dimers (**7–11**) are collected in Table I. The $^{31}P\{^1H\}$ NMR spectra display a low-field triplet assigned to the bridging S_2PR_2 groups and a high-field triplet attributable to the phosphine ligands. These data reveal that the magnitude of $^3J_{PP}$, the coupling between the phosphine and dithiophosphinate groups, steadily increases as the basicity of the axially bound phosphines is increased. In contrast, replacing methyl groups in the dithiophosphinate bridges with phenyl groups has little effect upon $^3J_{PP}$, as is shown by the pair of compounds $[Ru_2(CO)_4(\mu\text{-}S_2PMe_2)_2(PPh_3)_2]$ (**7**) and $[Ru_2(CO)_4(\mu\text{-}S_2PPh_2)_2(PPh_3)_2]$ (**11**), which have $^3J_{PP}$ values of 57 and 58 Hz, respectively. The axial and equatorial methyl groups of the bridging S_2PMe_2 ligands in complexes **7–10** appear as two doublets in the ^1H NMR spectrum between δ 1.8 and 2.3, with $^2J_{PH} \cong 12$ Hz. The $^{13}C\{^1H\}$ NMR spectra yield complementary information, showing two doublets between δ 30 and 32 ($^1J_{PC} \cong 51$ Hz) for the two different types of methyl carbons in the dithiophosphinate bridges. The carbonyl regions for these compounds contain only a singlet between δ 203 and 205 with no evidence of coupling to the phosphine ligands, unlike the $[Ru_2(CO)_4(\mu\text{-}O_2CMe)_2(PR'_2R'')_2]$ precursors, for which the carbonyl resonances appear as virtual triplets with a splitting of $^1/_2[^2J_{PC} + {}^3J_{PC}]$.

The IR data for compounds **7–11** are summarized in Table I, while that for the starting dimers (**2–6**) are again provided as supplementary material. All of the dithiophosphinate-bridged complexes display a four-band pattern between 1890 and 2020 cm^{-1}, which is typical of a sawhorse structure and quite comparable to the spectra of the acetate-bridged precursors. All of the IR spectra, except that for compound **9**, display two new bands between 510 and 555 cm^{-1}, which are assigned to the symmetric and antisymmetric stretches of the bridging dithiophosphinate groups. Complex **9**, $[Ru_2(CO)_4(\mu\text{-}S_2PMe_2)_2(PMe_2Ph)_2]$, displays just one band at 550 cm^{-1} and has an unusually low ^{31}P chemical shift for its bridging dithiophosphinate groups (δ 77.93 (t)) compared to those of compounds **7**, **8**, and **10**, which have resonances for the bridging S_2PMe_2 groups at ca. δ 99. It is not clear whether these spectral differences correspond to structural differences between the species, although the almost superimposable carbonyl regions of the ^{13}C NMR spectra suggest that any such differences will be subtle.

The structure determination of **7** confirms that the dithiophosphinate groups both bridge the two Ru(I) centers, as shown in Figure 1, giving the molecule a distorted sawhorse structure. The sulfur atoms of the $\mu\text{-}S_2PMe_2$ ligands are bonded opposite the carbonyl ligands, with the PPh_3 groups in the axial sites. Unlike the previous sawhorse complexes, which have the carbonyls on adjacent metals close to being eclipsed, the present structure is twisted by ca. 39° about the Ru–Ru bond. The twisting of this molecule seems to be the result of a complex interplay of effects within the dithiophosphinate groups and the Ru_2 core, which is presumably optimized at this highly strained arrangement. Surprisingly, in the present compound the S–P–S angles within the dithiophosphinate ligands (118.2 (1) and 118.4 (1)°) are very large, resulting in large bite distances (3.445 (2) and 3.444 (2) Å). By comparison, in $[Mo_2(\mu\text{-}S_2PEt_2)_4]\cdot THF$[25] and $[Mo_2(\mu\text{-}S_2PEt_2)_4(\eta^2\text{-}S_2PEt_2)_2]$[25] the S–P–S angles appear as expected, within the range 110.8–111.0°, yielding bite distances of 3.33 and 3.32 Å, respectively. Thus, it appears that the $Ru_2(CO)_4(PPh_3)_2$ unit is, at least partially, responsible for opening up the S–P–S angle. If the twisting of the molecule and the large Ru–Ru separation are solely a consequence of the large ligand bite, however, it is difficult to see why the S–P–S angle should be so large, since a smaller angle would reduce the bite and the resulting strain.

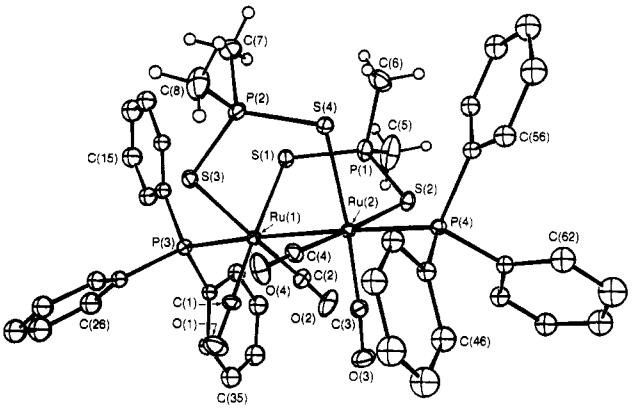

Figure 1. Perspective view of $[Ru_2(CO)_4(\mu\text{-}S_2PMe_2)_2(PPh_3)_2]\cdot{}^1/_2CH_2Cl_2$ (**7**), showing the numbering scheme. Thermal parameters are shown at the 20% level, except for the hydrogens, which are drawn artificially small for the methyl groups and have been omitted for the phenyl groups. The cocrystallized dichloromethane is not shown.

The two Ru–P distances, 2.402 (1) and 2.414 (2) Å, are comparable to those previously reported for $[Ru_2(CO)_4(\mu\text{-pz})_2(PPh_3)_2]$ and $[Ru_2(CO)_4(\mu\text{-}OC_5H_4N)_2(PPh_3)_2]$ (pz = pyrazolate, OC_5H_4N = oxypyridinate).[26] The two equatorial planes show very little tilt and are, in fact, inclined away from each other by about 3°; in other sawhorse structures these planes tilt toward each other because of the smaller bridging groups. The distortion from idealized octahedral geometry about each Ru atom is quite small, with the largest deviation being observed between the two dimetalladithiophosphinate rings, which have a dihedral angle of 93.27 (6)°. The average Ru–S bond length, 2.487 (2) Å, is slightly longer than the Ru–S bonds (average 2.447 (5) Å) trans to the carbonyl ligands in the closely related mercaptobenzothiazolinate-bridged complex $[Ru_2(CO)_4(mtb)_2(py)_2]$.[37] The P–S distances (average 2.006 (2) Å) for the bridging S_2PMe_2 groups fall in the range observed for both the bridging[23] and chelating[11] modes of the dithiophosphinate ligand.

Protonation of the Ru–Ru bond in **7** and **8** is facile, yielding the binuclear Ru(II)/Ru(II) species $[Ru_2(CO)_4(\mu\text{-H})(\mu\text{-}S_2PMe_2)_2(PPh_2R)_2][BF_4]$ (R = Ph (**12**), R = Me (**13**)) upon reaction with 1 molar equiv of $HBF_4\cdot OEt_2$ in dichloromethane. The relative ease with which the protonation reaction occurs may be facilitated by the reduction of strain that would be expected to occur by the lengthening of the Ru–Ru bond upon protonation. Reaction of the protonated species with the strong base NaH regenerates the starting complexes, **7** and **8**. However, weaker more conventional bases, such as NEt_3 and NEt_2H, do not reverse the protonations. By comparison, when strong acids are added to the μ-acetate precursors, $[Ru_2(CO)_4(\mu\text{-}O_2CMe)_2(PR'_2R'')_2]$, the proton appears to attack one of the more basic acetate oxygens rather than the Ru–Ru bond.[38]

The room-temperature $^{31}P\{^1H\}$ NMR spectra (Table I) for compounds **12** and **13** each display a high-field and a low-field triplet. The signal for the PPh_2R phosphorus nucleus is shifted downfield relative to the unprotonated parent compounds. For example, the PPh_3 signal in complex **12** is 17.94 ppm downfield from the PPh_3 signal in complex **7**. In contrast, the ^{31}P resonance of $\mu\text{-}S_2PMe_2$ moves to higher field upon protonation, as is shown by the pair of compounds $[Ru_2(CO)_4(\mu\text{-}S_2PMe_2)_2(PPh_3)_2]$ (**7**) (δ 97.51) and $[Ru_2(CO)_4(\mu\text{-H})(\mu\text{-}S_2PMe_2)_2(PPh_3)_2][BF_4]$ (**12**) (δ 89.33). Protonation also causes a sharp decrease in the

(37) Jeannin, S.; Jeannin, Y.; Lavigne, G. *Trans. Met. Chem.* **1976**, *1*, 186.
(38) Unpublished work, S. J. Sherlock, The University of Alberta, Edmonton, Alberta.

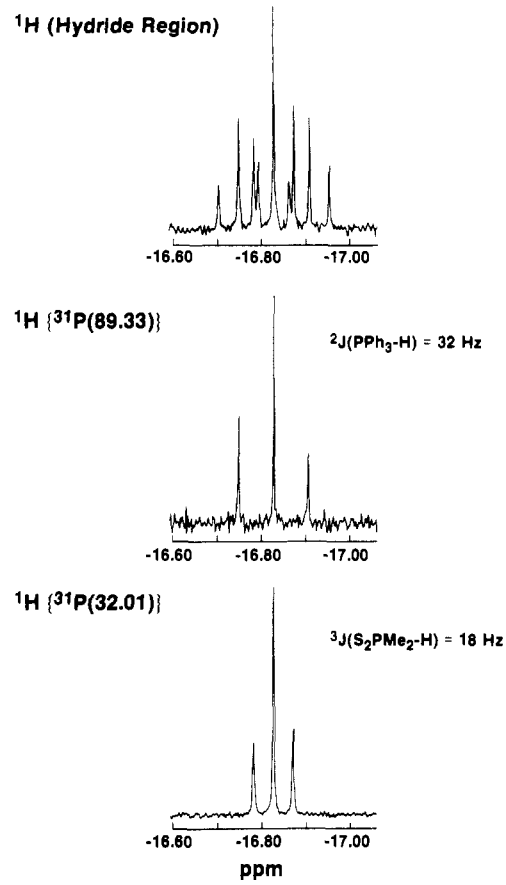

Figure 2. $^1H\{^{31}P\}$ Heteronuclear decoupling experiments performed upon the high-field resonance of $[Ru_2(CO)_4(\mu\text{-}H)(\mu\text{-}S_2PMe_2)_2(PPh_3)_2][BF_4]$ (**12**) in $CDCl_3$.

three-bond ^{31}P–^{31}P coupling. For example, $^3J_{PP}$ drops from 57 to 26 Hz when compound **7** is protonated. This can be compared with a previous study which found that $^3J_{PP}$ decreased by 13.3 Hz when the mixed-phosphine compound $[Os_2(CO)_4(\mu\text{-}O_2CMe)_2(PMe_2Ph)(PPh_3)]$ was converted to $[Os_2(CO)_4(\mu\text{-}H)(\mu\text{-}O_2CMe)_2(PMe_2Ph)(PPh_3)][PF_6]$ by treatment with $CF_3CO\text{-}OH$ and then NH_4PF_6.[39]

The ^1H NMR spectra of the protonated products, **12** and **13**, each contain a hydride resonance between δ −16 and −17, which appears as a triplet of triplets down to −80 °C, as expected for a hydride ligand coupled to both the phosphine and the dithiophosphinate groups. Selective $^1H\{^{31}P\}$ decoupling experiments performed upon $[Ru_2(CO)_4(\mu\text{-}H)(\mu\text{-}S_2PMe_2)_2(PPh_3)_2][BF_4]$ (**12**) established the larger coupling as $^3J_{PPh_3-H}$ (see Figure 2).

The tetrafluoroborate salts, **12** and **13**, both show an increase in the frequencies for the carbonyl stretches compared to those of the precursors and the typical broad band due to BF_4^- at ca. 1050 cm^{-1} in their IR spectra, supporting a cationic formulation for the diruthenium unit.

Although the $[Au(PPh_3)]^+$ cation is isolobal with H^+ and has previously displayed a similar tendency to attack metal–metal bonds,[40] it failed to react with compound **7**. Presumably, steric congestion about the Ru(I) centers and the relatively large size of the $[Au(PPh_3)]^+$ electrophile prevent coordination.

In order to further probe the reactivity of the Ru–Ru bond in complexes **7** and **8**, the reactions with diazomethane and dimethyl acetylenedicarboxylate were investigated. ^{31}P NMR spectroscopy revealed that neither of these reagents, even when used in excess, would react with complexes **7** and **8**. This lack of reactivity is probably the result of the coordinative saturation at the Ru(I) centers.

(39) Bates, P. A.; Deeming, A. J.; Hursthouse, M. B.; Randle, N. P. *J. Chem. Soc., Dalton Trans.* **1988**, 2753.
(40) Schiavo, S. L.; Bruno, G.; Nicolo, F.; Piraino, P.; Faraone, F. *Organometallics* **1985**, *4*, 2091.

In principle, $[Ru_2(CO)_4(\mu\text{-}OCMe)_2(NCMe)_2]$ (**1**) should also offer a route into dithiophosphinate-bridged complexes of Ru(I) via replacement of the bridging acetate groups. Replacement of the labile acetonitrile ligands in these products would then be expected to yield a large number of related species. Surprisingly, this route does not provide binuclear Ru(I) species but instead gives the known mononuclear Ru(II) species $[Ru(CO)_2(\eta^2\text{-}S_2PMe_2)_2]$[1] (**14**), containing chelating S_2PMe_2 groups, as shown in eq 1. If only 2 molar equiv of the dithiophosphinate salt is

$$6NaS_2PMe_2 + [Ru_2(CO)_4(\mu\text{-}O_2CMe)_2(NCMe)_2] \xrightarrow[23\ °C]{THF} 2Na_2S + 2MeCN + 2[Ru(CO)_2(\eta^2\text{-}S_2PMe_2)_2] + 2NaO_2CMe + Me_2P(S)P(S)Me_2 \quad (1)$$

used, as in the original attempt, compound **14** is still obtained, although in proportionally lower yield. The $^{31}P\{^1H\}$ NMR spectrum of the reaction mixture displays two singlets at δ 92.96 and 35.21, which have been assigned as due to $[Ru(CO)_2(\eta^2\text{-}S_2PMe_2)_2]$ (**14**) and $Me_2P(S)P(S)Me_2$, respectively, on the basis of previous work.[1,28-30] Orange-brown crystals of $[Ru(CO)_2(\eta^2\text{-}S_2PMe_2)_2]$ (**14**) were grown from toluene/diethyl ether, following extraction of this species with dichloromethane. The yellow residue that did not dissolve in dichloromethane was shown by IR spectroscopy to contain NaO_2CMe. Na_2S was not detected but presumably is present in the yellow residue along with the NaO_2CMe. The pale yellow supernatant left over from the recrystallization of **14** was found to contain mostly $Me_2P(S)P\text{-}(S)Me_2$. The ^1H NMR spectrum of $Me_2P(S)P(S)Me_2$ consists of a complex second-order multiplet at δ 1.93 in which the separation between the two most intense peaks of the multiplet is 6 Hz. This pattern is typical for a methyl-substituted diphosphine compound containing a P–P bond.[28]

Conclusions

The acetate-bridged species $[Ru_2(CO)_4(\mu\text{-}O_2CMe)_2(PR'_2R'')_2]$ have been established as useful precursors to an unusual class of dithiophosphinate-bridged Ru(I) complexes. These species appear to be the first group 8 metal complexes to contain bridging dithiophosphinate ligands. Although the X-ray structure of $[Ru_2(CO)_4(\mu\text{-}S_2PMe_2)_2(PPh_3)_2]$ indicates substantial strain and a long Ru–Ru bond, attempts to obtain products of methylene or alkyne insertion into the metal–metal bond have failed, presumably because the Ru metals are coordinatively saturated. The electrophilic reagent $HBF_4\cdot Et_2O$ does react with the neutral S_2PMe_2-bridged dimers to give the expected cationic, bridging hydride complexes, but the isolobal gold compound $[Au(PPh_3)][BF_4]$ failed to add to the Ru–Ru bond, presumably owing to steric congestion about the Ru metals.

The labile complex $[Ru_2(CO)_4(\mu\text{-}O_2CMe)_2(NCMe)_2]$ proved to be ill-suited as a precursor to a new series of dithiophosphinate-bridged Ru(I) dimers, since, in the presence of NaS_2PMe_2, the acetonitrile dimer is cleaved and oxidized to give the monomeric Ru(II) complex $[Ru(CO)_2(\eta^2\text{-}S_2PMe_2)_2]$, along with Na_2S, NaO_2CMe, MeCN, and $Me_2P(S)P(S)Me_2$. In contrast, the related complex $[Ru_2(CO)_4(\mu\text{-}O_2CMe)_2(PPh_3)_2]$ gives only $[Ru_2(CO)_4(\mu\text{-}S_2PMe_2)_2(PPh_3)_2]$ when reacted with an excess of NaS_2PMe_2.

Acknowledgment. We thank the Natural Sciences and Engineering Research Council (NSERC) of Canada and The University of Alberta for financial support. Funding for the PE 883 IR spectrometer and partial funding for the X-ray diffractometer were also provided by NSERC.

Supplementary Material Available: Tables of $^{31}P\{^1H\}$ and ^1H NMR data for the carboxylate-bridged Ru dimers and dithiophosphinate salts, $^{13}C\{^1H\}$ NMR data for the carboxylate-bridged Ru dimers and the dithiophosphinate salts, selected infrared data for the carboxylate-bridged Ru dimers, crystal data and details of intensity collection for $[Ru_2(CO)_4(\mu\text{-}S_2PMe_2)_2(PPh_3)_2]\cdot{}^1/_2CH_2Cl_2$, anisotropic thermal parameters, positional and thermal parameters for the hydrogen atoms, and bond lengths and angles within the phenyl groups and solvent molecules (13 pages); a listing of structure factors (30 pages). Ordering information is given on any current masthead page.